

Finite-momentum superconducting states due to odd-frequency Cooper pairing correlations

Takumi Sato¹, Satoru Hayami¹, Shingo Kobayashi², and Yasuhiro Asano³

¹*Graduate School of Science, Hokkaido University,
Sapporo 060-0810, Japan*

²*RIKEN Center for Emergent Matter Science,
Wako, Saitama 351-0198, Japan*

³*Department of Applied Physics,
Hokkaido University, Sapporo 060-8628, Japan.*

(Dated: May 25, 2026)

This paper discusses the origin of a nonuniform superconducting state in which Cooper pairs have a small but finite center-of-mass momentum. We analyze the instability of the normal state to such finite-momentum states using the pole of the pair fluctuation propagator in weak-coupling superconductors. The finite-momentum superconducting state is realized when the odd-frequency pairing correlations in the uniform superconducting state are expected to have sufficiently large amplitudes. We provide a perspective for a comprehensive understanding of inhomogeneous superconductivity and related phenomena.

I. INTRODUCTION

The Fulde-Ferrell-Larkin-Ovchinnikov (FFLO) state is a possible superconducting state in a conventional superconductor (SC) under a Zeeman field [1, 2]. In this state, Cooper pairs have a finite center-of-mass momentum \mathbf{q} because a Zeeman field lifts the degeneracy of the Kramers partners. As a result, the pair potential oscillates in real space with a period much longer than the Fermi wavelength. In what follows, we refer to such a nonuniform superconducting state as a finite-momentum superconducting state. Time-reversal symmetry (TRS)-breaking fields in the normal state have been regarded as an important element for the finite-momentum superconducting states [3–5]. Indeed, the superconducting diode effect has been actively discussed as a related phenomenon to the FFLO state [6–10]. However, other theoretical studies have suggested the possibility of the finite-momentum states in TRS-preserving SCs such as noncentrosymmetric SCs and $j = 3/2$ SCs [11, 12]. A common feature of these materials is that an electron has internal degrees of freedom such as spin, sublattice, band, and orbital. Unfortunately, our understanding of this issue is still limited. For instance, the results for a $j = 3/2$ SC suggest a positive correlation between the amplitude of interband Cooper pairs, which are composed of two electrons in different bands, and the emergence of finite-momentum states. In contrast, another theory does not indicate such correlations [13]. Thus, the role of such interband/interorbital Cooper pairs in forming finite-momentum states remains unclear. A more comprehensive physical picture that explains the mechanisms for stabilizing finite-momentum superconducting states is therefore desirable. We address this issue in the present paper.

Another prominent example of finite-momentum superconductivity is the pair density wave (PDW) state proposed, for example, in cuprates [14, 15]. Fermi sur-

face nesting plays a crucial role in stabilizing such spatially oscillating superconducting states. As a result, the center-of-mass momentum of a Cooper pair is comparable to the Fermi wavenumber, (i.e., $q \sim k_F$). The PDW states are therefore beyond the scope of this paper because the mechanisms underlying them are qualitatively different from those discussed here. In fact, we will show that the amplitude of the center-of-mass momentum in finite-momentum superconducting states is much smaller than the Fermi wavenumber, (i.e., $q \ll k_F$).

To clarify the problem, we summarize the common features among inhomogeneous superconducting states near a vortex core [16], those near a magnetic impurity (cluster) [17–21], and those at the surface of an unconventional SC [22, 23]. These theoretical studies have indicated the existence of odd-frequency Cooper pairs [24–29] around the inhomogeneous regions. Odd-frequency Cooper pairs appear as induced subdominant pairing correlations by the local defects. In the bulk region, where the superconducting state is almost uniform, conventional even-frequency Cooper pairs form the pair potential and stabilize the superconducting state. Namely, the pair potential itself belongs to conventional even-parity spin-singlet or odd-parity spin-triplet classes. Odd-frequency pairs do not form any pair potentials because the corresponding attractive interactions are absent. The odd-frequency pairing correlation functions always constitute part of the solution of the Gor'kov equation in inhomogeneous SCs [30] and make the local superfluid density $n(\mathbf{r})$ negative due to their paramagnetic property [31–33]. The spatial variation of the pair potential increases the energy of $\Delta E(\mathbf{r}) \approx n(\mathbf{r}) \mathbf{q}^2/m$ locally, where \mathbf{q} and m are the momentum and the effective mass of a Cooper pair, respectively. When the odd-frequency correlations locally reduce the superfluid density $n(\mathbf{r})$, the energy cost decreases by such amount. Therefore, odd-frequency Cooper pairs represent and simultaneously support the local deformation of the superconducting condensate

around a defect. In what follows, we will show that this is also true for finite-momentum superconducting states in the bulk. The existence of odd-frequency pairing correlations in the bulk was first pointed out in uniform multiband/orbital SCs [34]. Odd-frequency correlations increase the free-energy and then decrease the transition temperature of uniform superconducting states because of their paramagnetic response [35]. The conclusions of these studies suggest that odd-frequency pairing correlations play a role in promoting the transition from a homogeneous superconducting state to an inhomogeneous one.

The mechanisms and the properties of finite-momentum superconducting states have already been explored from various viewpoints [1, 2, 11, 12, 36, 37]. The aim of this paper is to provide another physical picture that explains the mechanisms underlying the emergence of finite-momentum superconducting states in various SCs. To this end, we examine the instability of the normal state in the presence of an attractive interaction between two electrons [38] by calculating the pair fluctuation propagator $D_s(\mathbf{q})$ within the ladder approximation [39]. It is possible to calculate two transition temperatures from the poles of $D_s(\mathbf{q})$: the transition temperature to a uniform superconducting state T_0 and the transition temperature to a finite-momentum superconducting state T_q . The superconducting state with a higher transition temperature is more stable. To analyze the mechanisms stabilizing finite-momentum superconducting states with small q , we expand the denominator of the fluctuation propagator as $D_s^{-1}(\mathbf{q}) \propto a + Bq^2 = 0$. For $B > 0$, we find that $T_0 > T_q$, indicating the appearance of a uniform superconducting state. For $B < 0$, we find that $T_0 < T_q$, indicating the appearance of a finite-momentum superconducting state with q . A general relationship shows that the coefficient B is proportional to the Meissner kernel, or equivalently to the superfluid density Q , in a *uniform* superconducting state. We conclude that the sign change of Q due to the odd-frequency pairing correlations in a uniform state explains the instability of the uniform superconducting state and the emergence of finite-momentum states.

A. Outline of this paper

To clarify the logical flow leading to the conclusion, we explain in detail the role of each section of this paper.

In Sec. II, we show the existence of odd-frequency pairing correlations in several SCs such as a single-band SC with spin-dependent potentials, a two-band/two-orbital SC in the presence of band/orbital hybridization, and SCs in a vector potential. We discuss the necessary conditions for the emergence of odd-frequency pairs.

In Sec. III, we first derive a general expression for the pair fluctuation propagator $D_s(\mathbf{q})$, which is a theoretical tool for analyzing the stability of finite-momentum superconducting states. The transition temperature is

calculated from the solutions of $D_s^{-1}(\mathbf{q}) = 0$. We expand the propagator up to the second order in q as $D_s^{-1}(\mathbf{q}) = a + Bq^2$. The uniform superconducting state appears for $a = 0$ and $B > 0$, whereas the finite-momentum state with small q is more stable for $a > 0$ and $B < 0$. Our analytic calculation shows a proportional relationship between the coefficient B and the superfluid weight Q . Therefore, the finite-momentum superconducting states appear when the amplitude of the odd-frequency pairing correlations is large enough to change the sign of Q in the corresponding uniform state. This is the central conclusion of this paper. Although the validity of the theory is limited to sufficiently small $q \ll k_F$, the condition for the emergence of finite-momentum superconducting states can be applied to any SC.

In Sec. IV, we apply our theory to the well-known FFLO state in a conventional SC in Zeeman fields. We demonstrate that the odd-frequency spin-triplet s -wave correlation decreases the superfluid weight by using the analytic expression of Q . To check the validity of our theory in Sec. III, we solve the equation $D_s^{-1}(\mathbf{q}) = 0$ fully numerically and obtain the highest transition temperature T_q and the corresponding q . The numerical results show a transition to the FFLO state in Zeeman fields large enough to make $Q < 0$. All the numerical solutions for q in the FFLO state satisfy $q \ll k_F$. These results support the main conclusion.

In Sec. V, we apply our theory to two TRS-preserving SCs: a two-band SC with s -wave interband pairing order [40] and a $j = 3/2$ SC with s -wave pseudospin-quintet pairing order [41]. By solving $D_s^{-1}(\mathbf{q}) = 0$ numerically, we confirm that finite-momentum superconducting states with small q become more stable than the uniform state.

In Sec. VI, we discuss the possibility of finite-momentum superconducting states in real materials. Moreover, we briefly discuss the close relationship between the second-order transition to finite-momentum superconducting states and the first-order transition to the uniform state. The conclusion is given in Sec. VII.

Throughout this paper, we use the units of $k_B = c = \hbar = 1$ where k_B is the Boltzmann constant and c is the speed of light and $e < 0$ is the charge of an electron.

II. ODD-FREQUENCY PAIRING CORRELATIONS

In this section, we show the general condition for the appearance of odd-frequency pairing correlations and apply the condition to single-band SCs with spin-dependent potentials and to multiband/orbital SCs with band/orbital hybridization. The TRS-breaking fields have been considered as essential ingredients for realizing finite-momentum superconducting states. In fact, extensive theoretical and experimental research has been devoted to exploring superconducting states that survive under strong magnetic fields near the Pauli limit [42–44]. Here, we reconsider the importance of TRS-breaking

fields from the perspective of odd-frequency Cooper pairing.

Generally speaking, the Bogoliubov-de Gennes (BdG) Hamiltonian for uniform superconducting states takes the form

$$H_{\text{BdG}}(\mathbf{k}) = \begin{bmatrix} \hat{\xi}_{\mathbf{k}} & \hat{\Delta}(\mathbf{k}) \\ -\hat{\Delta}^*(-\mathbf{k}) & -\hat{\xi}_{-\mathbf{k}}^* \end{bmatrix}. \quad (1)$$

The anomalous Green's function, obtained as a solution of the Gor'kov equation, is formally expressed as

$$\hat{\mathcal{F}}(\mathbf{k}, i\omega_\ell) = \left[\hat{\Delta}(\mathbf{k})\hat{\Delta}^*(-\mathbf{k}) - \omega_\ell^2 - \hat{\Delta}(\mathbf{k})\hat{\xi}_{-\mathbf{k}}^*\hat{\Delta}^{-1}(\mathbf{k})\hat{\xi}_{\mathbf{k}} - i\omega_\ell\hat{P}_O(\mathbf{k})\hat{\Delta}^{-1}(\mathbf{k}) \right]^{-1} \hat{\Delta}(\mathbf{k}), \quad (2)$$

$$\hat{P}_O(\mathbf{k}) := \hat{\xi}_{\mathbf{k}}\hat{\Delta}(\mathbf{k}) - \hat{\Delta}(\mathbf{k})\hat{\xi}_{-\mathbf{k}}^*, \quad (3)$$

where $\hat{P}_O(\mathbf{k})$ characterizes the presence of odd-frequency pairing correlations [28, 45, 46]. When an attractive interaction works between the Kramers partners, the pair potential in the BdG Hamiltonian can be expressed as $\hat{\Delta}(\mathbf{k}) = \Delta(\mathbf{k})\hat{U}_T$ where $\Delta(\mathbf{k})$ is an even function of \mathbf{k} representing an even-parity superconductivity. The matrix \hat{U}_T is the unitary part of the time-reversal operator $\mathcal{T} = \hat{U}_T\mathcal{C}$, where \mathcal{C} denotes complex conjugation combined with the transformation $\mathbf{k} \rightarrow -\mathbf{k}$. The relation

$$\begin{aligned} \hat{P}_O(\mathbf{k}) &= \left[\hat{\xi}_{\mathbf{k}} - \hat{U}_T\hat{\xi}_{-\mathbf{k}}^*\hat{U}_T^{-1} \right] \hat{\Delta}(\mathbf{k}) \\ &= \left[\hat{\xi}_{\mathbf{k}} - \mathcal{T}\hat{\xi}_{\mathbf{k}}\mathcal{T}^{-1} \right] \hat{\Delta}(\mathbf{k}), \end{aligned} \quad (4)$$

indicates that TRS-breaking fields in the normal state Hamiltonian is necessary for the emergence of the odd-frequency pairing correlation.

To discuss the importance of TRS-breaking fields, we begin with spin-singlet even-parity SCs for spin $s = 1/2$ electrons, where \hat{U}_T is replaced by $i\hat{\sigma}_2$ with $\hat{\sigma} = (\hat{\sigma}_1, \hat{\sigma}_2, \hat{\sigma}_3)$ being the Pauli matrices in spin space. The normal state Hamiltonian includes two types of spin active potentials:

$$\hat{\xi}_{\mathbf{k}} = \xi_{\mathbf{k}} + \mathbf{h}_{\mathbf{k}} \cdot \hat{\sigma} + \boldsymbol{\lambda}_{\mathbf{k}} \cdot \hat{\sigma}. \quad (5)$$

The TRS-breaking fields $\mathbf{h}_{\mathbf{k}} = \mathbf{h}_{-\mathbf{k}}$ represent a Zeeman field, a ferromagnetic exchange field [42, 43, 47–49], and an alternating magnetic exchange field [50–69]. On the contrary, the potential $\boldsymbol{\lambda}_{\mathbf{k}} = -\boldsymbol{\lambda}_{-\mathbf{k}}$ represents antisymmetric spin-orbit interactions preserving TRS [70–72]. The relation in Eq. (4) shows that only $\mathbf{h}_{\mathbf{k}}$ induces the odd-frequency Cooper pairs in the spin-singlet SCs, as listed in the second row of Table I.

The TRS-breaking fields become less important in spin-triplet SCs described by the pair potential

$$\hat{\Delta}(\mathbf{k}) = \mathbf{d}_{\mathbf{k}} \cdot \hat{\sigma} i\hat{\sigma}_2, \quad (6)$$

with $\mathbf{d}_{\mathbf{k}} = -\mathbf{d}_{-\mathbf{k}}$. In a spin-triplet SC, two types of odd-frequency correlations exist, as listed in the third row

of Table I. One is the spin-singlet odd-parity correlation induced by the TRS-breaking field $\mathbf{h}_{\mathbf{k}}$ and the other is the spin-triplet even-parity correlation induced by the spin-orbit interactions $\boldsymbol{\lambda}_{\mathbf{k}}$ preserving TRS. The authors in Refs. [71, 72] show that $\boldsymbol{\lambda}_{\mathbf{k}} \times \mathbf{d}_{\mathbf{k}} = 0$ is necessary for realizing a stable superconducting state. Namely, T_c for $\boldsymbol{\lambda}_{\mathbf{k}} \times \mathbf{d}_{\mathbf{k}} = 0$ is higher than that for $\boldsymbol{\lambda}_{\mathbf{k}} \times \mathbf{d}_{\mathbf{k}} \neq 0$. The instability (stability) of superconducting states is explained well by the presence (absence) of odd-frequency Cooper pairs in the bulk [35].

The TRS-breaking fields are not a necessary item for the odd-frequency pairing correlations when an electron has extra internal degrees of freedom. To clarify this point, we consider a two-band SC, where the Pauli matrices $\hat{\rho}_i$ for $i = 1 - 3$ describe the 2×2 band space in the normal state Hamiltonian

$$\hat{\xi}_{\mathbf{k}} = \xi_{\mathbf{k}}\hat{\rho}_0 + V\hat{\rho}_1 + V'\hat{\rho}_2 + \varepsilon\hat{\rho}_3. \quad (7)$$

The potentials V and V' represent the band hybridization, and ε represents band asymmetry. The spin degree of freedom is omitted because the normal state Hamiltonian contains no spin active terms. The interband pair potential described by $\Delta\hat{\rho}_1$ represents a spin-singlet s -wave even-band-parity pair potential. In this case, Eq. (3) becomes $\hat{P}_O = 2i\Delta\varepsilon\hat{\rho}_2$, which indicates the emergence of odd-frequency odd-band-parity pairing correlations [34]. In Table. II, we summarize the matrix structures of the pair potentials and those of the induced odd-frequency correlations. For all even-band-parity pair potentials such as $\Delta\hat{\rho}_0$, $\Delta\hat{\rho}_1$, and $\Delta\hat{\rho}_3$, the band hybridization or asymmetry generates odd-frequency correlations belonging to the odd-band-parity symmetry class. When we consider an odd-band-parity pair potential, $\Delta\hat{\rho}_2$, the induced odd-frequency correlations belong to the even-band-parity class [34]. Therefore, the potentials that hybridize the internal degrees of freedom of electrons are crucial for the emergence of the odd-frequency pairing correlations.

Finally, we point out a trivial potential that generates odd-frequency pairing correlations. In the presence of a vector potential, the normal state Hamiltonian is given by

$$\hat{\xi}_{\mathbf{k}} = \xi_{\mathbf{k}} + \frac{e^2\mathbf{A}^2}{2m} - \frac{e\hbar}{m}\mathbf{A} \cdot \mathbf{k}. \quad (8)$$

Since a vector potential couples to the charge of an electron, $\hat{\xi}_{\mathbf{k}}$ is always proportional to the identity matrix in any internal spaces. We find that odd-frequency correlations characterized by $\hat{P}_O \propto e\mathbf{A} \cdot \mathbf{k}$ are induced, belonging to the parity opposite to that of the pair potential.

III. PAIR FLUCTUATION PROPAGATOR

In this section, we introduce a theoretical tool to discuss the instability of the normal state in the presence

TABLE I. The pair potentials and the induced odd-frequency pairing correlations are summarized for the single band $s = 1/2$ SCs. The normal state Hamiltonian is given in Eq. (5).

Pair potential	\hat{P}_O
$\Delta_{\mathbf{k}} i\hat{\sigma}_2$	$2\Delta_{\mathbf{k}} \mathbf{h}_{\mathbf{k}} \cdot \hat{\sigma} i\hat{\sigma}_2$
$\mathbf{d}_{\mathbf{k}} \cdot \hat{\sigma} i\hat{\sigma}_2$	$2[\mathbf{d}_{\mathbf{k}} \cdot \mathbf{h}_{\mathbf{k}} + i(\boldsymbol{\lambda}_{\mathbf{k}} \times \mathbf{d}_{\mathbf{k}}) \cdot \hat{\sigma}] i\hat{\sigma}_2$

TABLE II. The pair potentials and the induced odd-frequency pairing correlations are summarized for the two-band SCs. The normal state Hamiltonian is given in Eq. (7).

Pair potential	\hat{P}_O
$\Delta \hat{\rho}_0$	$2\Delta V' \hat{\rho}_2$
$\Delta \hat{\rho}_1$	$2i\Delta \varepsilon \hat{\rho}_2$
$\Delta \hat{\rho}_2$	$2\Delta(V' \hat{\rho}_0 - i\varepsilon \hat{\rho}_1 + iV \hat{\rho}_3)$
$\Delta \hat{\rho}_3$	$-2i\Delta V \hat{\rho}_2$

of attractive interactions between two electrons. The Hamiltonian describing such electronic states is given by

$$\mathcal{H} = \mathcal{H}_0 + \mathcal{H}_1, \quad (9)$$

$$\mathcal{H}_0 = \sum_{\mathbf{k}\alpha\beta} \xi_{\mathbf{k}\alpha\beta} c_{\mathbf{k}\alpha}^\dagger c_{\mathbf{k}\beta}, \quad \xi_{\mathbf{k}\alpha\beta} = \epsilon_{\mathbf{k}\alpha\beta} - \mu \delta_{\alpha\beta}, \quad (10)$$

$$\mathcal{H}_1 = -g \sum_{\mathbf{q}} \Phi_{\mathbf{q}}^\dagger \Phi_{\mathbf{q}}, \quad (11)$$

$$\Phi_{\mathbf{q}} = \frac{1}{\sqrt{2N}} \sum_{\mathbf{k}'\gamma\delta} w_{\gamma\delta}^*(\mathbf{k}') c_{\mathbf{k}'+\frac{\mathbf{q}}{2}\gamma} c_{-\mathbf{k}'+\frac{\mathbf{q}}{2}\delta}, \quad (12)$$

where $\alpha, \beta, \gamma, \delta$ denote the internal degrees of freedom of an electron, such as spin, band, orbital, and sublattice, $c_{\mathbf{k}\alpha}$ is the annihilation operator of an electron with \mathbf{k} and α , and $g > 0$ represents the strength of the attractive interaction. $\Phi_{\mathbf{q}}$ is the annihilation operator of a

Cooper pair with center-of-mass momentum \mathbf{q} , and N is the number of unit cells in the underlying lattice. The attractive interaction is characterized by $w_{\sigma\sigma'}(\mathbf{k})$, which satisfies $w_{\sigma\sigma'}(\mathbf{k}) = -w_{\sigma'\sigma}(-\mathbf{k})$ due to the fermionic anticommutation relations.

Within the linear response theory [39], the transition from the normal state to the superconducting state is examined by analyzing the pole of the pair fluctuation propagator, which is defined as

$$D_s(\mathbf{q}, i\nu_n) := - \int_0^{1/T} d\tau \langle T_\tau \Phi_{\mathbf{q}}(\tau) \Phi_{\mathbf{q}}^\dagger \rangle e^{i\nu_n \tau}, \quad (13)$$

with $\Phi_{\mathbf{q}}(\tau) = e^{\tau\mathcal{H}} \Phi_{\mathbf{q}} e^{-\tau\mathcal{H}}$, where $\nu_n = 2n\pi T$ is the bosonic Matsubara frequency with n and T being an integer number and a temperature, respectively. By summing the ladder diagrams, we obtain

$$D_s(\mathbf{q}, i\nu_n) = \frac{-\Pi_{s0}(\mathbf{q}, i\nu_n)}{1 - g\Pi_{s0}(\mathbf{q}, i\nu_n)}, \quad (14)$$

$$\begin{aligned} \Pi_{s0}(\mathbf{q}, i\nu_n) = & -T \sum_{\omega_\ell} \frac{1}{N} \sum_{\mathbf{k}} \text{Tr} \left[\hat{\mathcal{G}}_0(\mathbf{k} + \mathbf{q}/2, i\omega_\ell) \hat{w}(\mathbf{k}) \right. \\ & \left. \times \hat{\mathcal{G}}_0(\mathbf{k} - \mathbf{q}/2, i\omega_\ell - i\nu_n) \hat{w}^\dagger(\mathbf{k}) \right], \end{aligned} \quad (15)$$

where $\hat{\mathcal{G}}_0(\mathbf{k}, i\omega_\ell) = [i\omega_\ell - \hat{\xi}_{\mathbf{k}}]^{-1}$ is the Green's function in the absence of the attractive interaction, $\underline{X}(\mathbf{k}, i\omega_\ell) := -X^*(-\mathbf{k}, i\omega_\ell)$ represents particle-hole conjugation of a function $X(\mathbf{k}, i\omega_\ell)$ and $\omega_\ell = (2\ell + 1)\pi T$ is the fermionic Matsubara frequency with ℓ being an integer number. The second-order transition to a superconducting phase is characterized by the divergence of the retarded propagator $D_s^R(\mathbf{q}, \omega) := D_s(\mathbf{q}, i\nu_n \rightarrow \omega + i\delta)$. In the following, we put $\omega = 0$, since we focus on static superconducting states. To discuss the transition to finite-momentum superconducting states with small q , we expand the pair polarization function $\Pi_{s0}^R(\mathbf{q}, 0) := \Pi_{s0}(\mathbf{q}, i\nu_n \rightarrow \omega + i\delta = 0)$ with respect to \mathbf{q} :

$$\begin{aligned} \Pi_{s0}^R(\mathbf{q}, 0) = & -T \sum_{\omega_\ell} \frac{1}{N} \sum_{\mathbf{k}} \text{Tr} \left[\hat{\mathcal{G}}_0 \hat{w} \hat{\mathcal{G}}_0 \hat{w} \right. \\ & - \frac{q_\mu q_\nu}{4} \text{Re} \left[\partial_{k_\mu} \partial_{k_\nu} \hat{\xi} \hat{\mathcal{G}}_0 \hat{w} \hat{\mathcal{G}}_0 \hat{w} \hat{\mathcal{G}}_0 + \hat{v}_\mu \hat{\mathcal{G}}_0 \hat{v}_\nu \hat{\mathcal{G}}_0 \hat{w} \hat{\mathcal{G}}_0 \hat{w} \hat{\mathcal{G}}_0 + \hat{v}_\mu \hat{\mathcal{G}}_0 \hat{w} \hat{\mathcal{G}}_0 \hat{w} \hat{\mathcal{G}}_0 \hat{v}_\nu \hat{\mathcal{G}}_0 + \hat{v}_\mu \hat{\mathcal{G}}_0 \hat{w} \hat{\mathcal{G}}_0 \hat{v}_\nu \hat{\mathcal{G}}_0 \hat{w} \hat{\mathcal{G}}_0 \right] \\ & \left. + O(q^4) \right], \end{aligned} \quad (16)$$

where the repeated indices $\mu, \nu = x, y, z$ are summed over, $\partial_{k_\mu} f g = \frac{\partial f}{\partial k_\mu} g$, $\hat{v}_\mu := \partial_{k_\mu} \hat{\xi}$ is the velocity operator, and $\hat{\mathcal{G}}_0, \hat{w}, \hat{w}$, and \hat{v}_μ are abbreviations of $\hat{\mathcal{G}}_0(\mathbf{k}, i\omega_\ell), \hat{w}(\mathbf{k}), -\hat{w}^*(-\mathbf{k})$, and $-\hat{v}_\mu^*(-\mathbf{k})$, respectively. We adopt the lattice constant as the length unit. In Eq. (16), we

have assumed that the odd-order terms with respect to \mathbf{q} vanish for simplicity [73].

After some algebra, the pair fluctuation propagator can be expressed in terms of the Meissner kernel in the uni-

form superconducting state:

$$[D_s^R(\mathbf{q}, 0)]^{-1} \propto \frac{1}{g} - \Pi_{s0}^R(\mathbf{q}, 0) \\ = a(T) + B_{\mu\nu}(T)q_\mu q_\nu + O(q^4), \quad (17)$$

$$a(T) = \frac{1}{g} + T \sum_{\omega_\ell} \frac{1}{N} \sum_{\mathbf{k}} \text{Tr} \left[\hat{\mathcal{G}}_0 \hat{w} \hat{\mathcal{G}}_0 \hat{w} \right], \quad (18)$$

$$B_{\mu\nu}(T) = \left. \frac{K_{\mu\nu}(\mathbf{0}, 0)}{4e^2\alpha^2|\Delta|^2} \right|_{\Delta=0}, \quad (19)$$

where $a(T)$ and $K_{\mu\nu}(\mathbf{0}, 0)$ correspond to the quadratic coefficient of the Ginzburg-Landau (GL) free-energy and the Meissner kernel for a uniform superconducting state, respectively. The last relation between $B_{\mu\nu}(T)$ and $K_{\mu\nu}(\mathbf{0}, 0)$ is particularly important to understand how odd-frequency pairing correlations destabilize a uniform superconducting state. The derivation of the Meissner kernel is presented in Appendix. A. According to the definition in Eq. (A18), the pair potential can be represented as

$$\hat{\Delta}(\mathbf{k}) = \alpha \Delta \hat{w}(\mathbf{k}), \quad (20)$$

with constants $\alpha \in \mathbb{R}$ and $\Delta \in \mathbb{C}$. By substituting the expression in Eq. (20) into Eq. (A21) and comparing the result with the second term in Eq. (16), we obtain the relation in Eq. (19).

Moreover, without loss of generality, the GL free-energy of a uniform superconducting state can be written as

$$\Omega_{\text{GL}}(\Delta) = a(T) |\Delta|^2 + b(T) |\Delta|^4 + O(\Delta^6). \quad (21)$$

The transition temperature to a uniform superconducting state T_0 is given by

$$a(T_0) = 0, \quad (22)$$

since $a(T)$ changes the sign at $T = T_0$. The kind of the transition is characterized by the sign of $b(T_0)$. The transition to the uniform superconducting state is a second-order (continuous) for $b > 0$, whereas it is a first-order (discontinuous) for $b < 0$.

Using Eq. (17), the transition temperature to a finite-momentum state $T_{\mathbf{q}}$ is calculated from

$$a(T_{\mathbf{q}}) + B_{\mu\nu}(T_{\mathbf{q}})q_\mu q_\nu = 0. \quad (23)$$

We assume that q is much smaller than k_F so that fourth- and higher-order terms can be neglected. To satisfy Eq. (23), the two cases are possible:

$$(i) \ a(T_{\mathbf{q}}) < 0 \text{ and } B_{\mu\nu}(T_{\mathbf{q}})q_\mu q_\nu > 0,$$

$$(ii) \ a(T_{\mathbf{q}}) > 0 \text{ and } B_{\mu\nu}(T_{\mathbf{q}})q_\mu q_\nu < 0.$$

Case (i) gives $T_{\mathbf{q}} < T_0$, indicating that the uniform superconducting state is more stable than the finite-momentum states. As a result, the transition to the uniform superconducting state occurs at $T = T_0$. Case

(ii) gives $T_{\mathbf{q}} > T_0$, indicating that the transition to a finite-momentum state occurs at $T = T_{\mathbf{q}}$. In this way, the stability of the inhomogeneous superconducting state is determined. These conclusions hold true as long as the higher-order terms $O(q^4)$ in Eq. (17) are negligible. The even- (odd-) frequency pairing correlations contribute positively (negatively) to the Meissner kernel in Eq. (19) [35]. Therefore, the stability of a superconducting state is determined by the relative amplitude between the even- and the odd-frequency pairing correlations. We also find that b in Eq. (21) and $B_{\mu\nu}$ have the same sign in many cases. This suggests a close relationship between the continuous transition to a finite-momentum state and the discontinuous transition to a uniform state. We will discuss this issue in Sec. VI.

At the end of this section, we briefly explain how the theory in this section connects with the results in the following sections. In Sec. IV, we apply the argument to the FFLO state in a spin-singlet s -wave SC in Zeeman fields. The transition to the FFLO state due to the TRS-breaking field is described well by the theory. Although we neglect higher order terms in Eq. (17), fully numerical solution of $[D_s^R]^{-1} = 0$ gives finite-momentum states with $q \ll k_F$. In Sec. V, we seek the possibility of finite-momentum states in two-band SCs and $j = 3/2$ SCs that preserve TRS. The numerical results indicate the presence of finite-momentum superconducting state with $q \ll k_F$.

IV. FFLO STATE

In this section, we apply the theory in Sec. III to the FFLO state in a conventional SC [1, 2]. We consider spin-singlet superconductivity under Zeeman fields on a square lattice. In Eq. (9), we choose

$$\hat{\xi}_{\mathbf{k}} = \xi_{\mathbf{k}} \hat{\sigma}_0 - \mathbf{h} \cdot \hat{\boldsymbol{\sigma}}, \quad \hat{w}(\mathbf{k}) = \frac{1}{\sqrt{2}}(i\hat{\sigma}_2), \quad (24)$$

$$\xi_{\mathbf{k}} = -2t(\cos k_x + \cos k_y) + 4t - \mu, \quad (25)$$

where $\mathbf{h} := \mu_B \mathbf{B}$ represents the Zeeman term, and $\hat{\sigma}_0$ is the unit matrix. The length is measured in units of the lattice constant $c_0 = 1$. The pair potential in the BdG Hamiltonian for the uniform phase is given by $\hat{\Delta}(\mathbf{k}) = \Delta(i\hat{\sigma}_2)$. To proceed with analytic calculations, we consider the continuum limit of the model: $\xi_{\mathbf{k}} \rightarrow (k_x^2 + k_y^2)/2m - \mu$ with $m = 1/2t$ and $\frac{1}{N} \sum_{\mathbf{k}} \rightarrow \frac{1}{V_{\text{vol}}} \sum_{\mathbf{k}}$, where V_{vol} denotes the volume of the system. By solving the Gor'kov equation in Eq. (A17), the anomalous Green's function is obtained as [13]

$$\hat{\mathcal{F}}_z(\mathbf{k}, i\omega_\ell) = \frac{-1}{Z_z} [\omega_\ell^2 + \xi_{\mathbf{k}}^2 + \Delta^2 - h^2 + 2i\omega_\ell \mathbf{h} \cdot \hat{\boldsymbol{\sigma}}] \Delta(i\hat{\sigma}_2), \quad (26)$$

$$Z_z = \xi_{\mathbf{k}}^4 + 2\xi_{\mathbf{k}}^2 A_z + C_z, \quad (27)$$

$$A_z = \omega_\ell^2 - h^2 + \Delta^2, \quad C_z = A_z^2 + 4\omega_\ell^2 h^2, \quad (28)$$

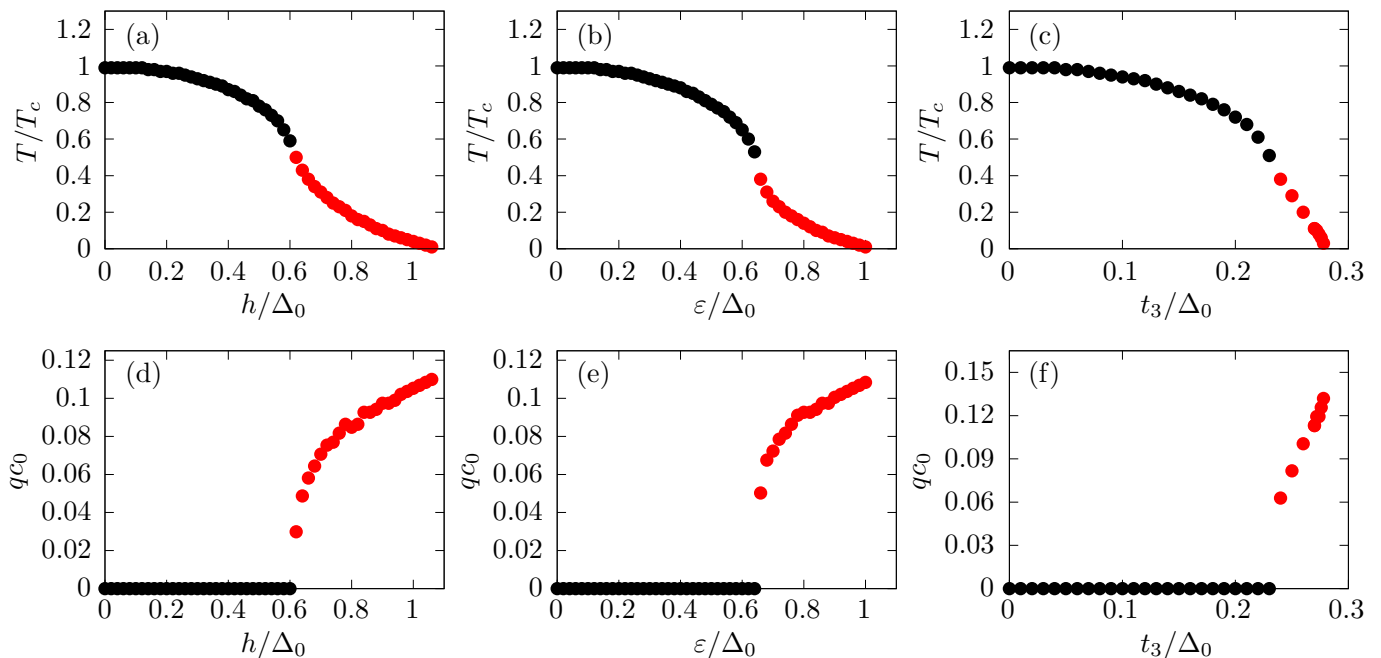


FIG. 1. The phase boundary between the normal and superconducting states is shown in (a)–(c), which is determined by the zeros of the denominator of the pair fluctuation propagator in Eq. (14) with Eq. (15). Panels (a), (b), and (c) show the results for a conventional SC under Zeeman fields in the h – T plane, a two-band SC with interband spin-singlet pairing order ($s = -1$) in the ε – T plane, and a $j = 3/2$ SC in the t_3 – T plane, respectively. The transition points to the uniform (finite-momentum) state are indicated by black (red) dots. Figures (d)–(f) show the center-of-mass momentum of the Cooper pair q at the transition point, and the dots are colored in the same manner as in (a)–(c).

where the last term in Eq. (26) represents the odd-frequency pairing correlation induced by the Zeeman field [49, 74]. The expression for the normal Green's function \hat{G}_z is presented in Appendix B. Using the obtained Green's function, the GL coefficient $a_z(T)$ and the Meissner kernel $K_{z,\mu\nu}$ are calculated as [13]

$$a_z(T) = \frac{1}{g} - N_0\pi T \sum_{\omega_\ell} \frac{\omega_\ell^2}{|\omega_\ell|(\omega_\ell^2 + h^2)}, \quad (29)$$

$$K_{z,\mu\nu}(\mathbf{0}, 0) = \delta_{\mu\nu} \frac{2ne^2}{m} Q_z, \quad (30)$$

$$Q_z = \sqrt{2\pi} T \sum_{\omega_\ell} \frac{\Delta^2 \{A_z^3 + \sqrt{C_z}(A_z^2 - 2\omega_\ell^2 h^2)\}}{[C_z(A_z + \sqrt{C_z})]^{3/2}}. \quad (31)$$

where $n = k_F^2/4\pi$ and $N_0 = n/\mu$ denote the electron density per spin and the density of states per spin, respectively. To obtain Eqs. (29) and (30), the momentum summation is replaced by an integration over ξ : $\frac{1}{V_{\text{vol}}} \sum_{\mathbf{k}} \rightarrow N_0 \int d\xi$. To derive Eq. (30), we subtract and add the diamagnetic contribution in the normal state to avoid the formal divergence of the integrand [75]. Equation (23) becomes

$$a(T_q) + \frac{nQ(T_q)}{4m|\Delta|^2} \Big|_{\Delta=0} q^2 = 0, \quad (32)$$

with $a = a_z$ and $Q = Q_z$ in the present case. In the Meissner kernel in Eq. (30), Q_z is called superfluid weight. The

last term in the numerator of Eq. (31), which stems from the last term in Eq. (26), represents the negative contribution of odd-frequency Cooper pairs to Q_z . Therefore, Eq. (32) has solutions with $q \neq 0$ when the superfluid weight changes the sign for large Zeeman fields [13].

To examine the above argument based on the theory in Sec. III, we solve $[D_s^R(\mathbf{q}, 0)]^{-1} = 0$ in Eq. (14) with Eq. (15) fully numerically for the tight-binding model with $\mathbf{q} = (q, 0)$. The solution on the h – T plane is shown in Fig. 1(a). Since $[D_s^R(\mathbf{q}, 0)]^{-1} = 0$ is a single equation for T_q and \mathbf{q} , we obtain a set of solutions (T_q, \mathbf{q}) . The highest transition temperatures are plotted in Fig. 1(a) and the corresponding q are plotted in (d). The vertical axis in (a) is normalized to T_c , the transition temperature at $h = 0$, and the horizontal axis is normalized to $\Delta_0 := \pi e^{-C} T_c = 1.76 T_c$, which is the amplitude of the pair potential at $h = T = 0$, with $C = 0.577$ being Euler's constant [76]. In the numerical simulation, we choose $\mu = t$ and $T_c = 0.05t$. For weak Zeeman fields, the transition to the uniform state with $q = 0$ occurs as shown with black dots in Figs. 1(a) and (d). When a Zeeman field goes beyond a critical value, finite-momentum superconducting states appear below T_q as shown with the red dots. The dependence of q on h in (d) shows that q increases monotonically with h . The transition temperature T_q decreases with increasing h and vanishes at $h \sim \Delta_0$. The phase boundary in Fig. 1(a) slightly deviates from that for a circular Fermi surface [44, 77]

because the direction $\mathbf{q} = (q, 0)$ satisfies a favorable nesting condition on the anisotropic Fermi surface [78–80]. The results in (d) show that q is much smaller than the Fermi wavenumber $k_F \sim 1/c_0$. This result, $(qc_0)^2 \ll 1$, justifies the expansion in Eq. (17).

The emergence of the FFLO state is usually considered as a result of the destruction of Cooper pairs composed of Kramers partners by TRS-breaking perturbations. This interpretation provides a clear physical picture of the phenomenon. However, Eqs. (31) and (32) suggest an alternative understanding of the FFLO state. In this picture, the uniform superconducting state is unstable because odd-frequency Cooper pairs decrease the superfluid density. This perspective can also explain the appearance of the FFLO states driven by vector potentials [81], as discussed at the end of Sec. II. Moreover, finite-momentum superconducting states can appear in TRS-preserving SCs because TRS-breaking fields are not essential for the emergence of odd-frequency Cooper pairs, as demonstrated in Sec. II. In the next section, we discuss two examples of such SCs.

V. TRS-PRESERVING FINITE-MOMENTUM STATES

In this section, we discuss two examples of finite-momentum superconducting states in TRS-preserving SCs. One is a two-band SC with interband pairing order, where odd-frequency pairing correlations are induced by band-hybridization and/or band-asymmetry. The other is a $j = 3/2$ SC with pseudospin-quintet pairing order, where spin-orbit interactions generate odd-frequency pairs.

A. Two-band SCs with interband pairing orders

We consider a two-band SC on a two-dimensional tight-binding square lattice. In Eq. (9), we choose

$$\hat{\xi}_{\mathbf{k}} = \xi_{\mathbf{k}}\hat{\rho}_0\hat{\sigma}_0 + \varepsilon\hat{\rho}_3\hat{\sigma}_0 + V\hat{\rho}_1\hat{\sigma}_0, \quad (33)$$

$$\xi_{\mathbf{k}} = -2t(\cos k_x + \cos k_y) + 4t - \mu, \quad (34)$$

$$\hat{w}(\mathbf{k}) = \begin{cases} \frac{1}{\sqrt{2}}(i\hat{\rho}_2)\hat{\sigma}_1 & (s = +1) \\ \frac{1}{\sqrt{2}}\hat{\rho}_1(i\hat{\sigma}_2) & (s = -1) \end{cases}. \quad (35)$$

The length is measured in units of the lattice constant $c_0 = 1$. The asymmetry and the hybridization between the two bands are represented by ε and V , respectively. The pair potential matrix with s -wave symmetry is given by

$$\hat{\Delta} = \begin{cases} \Delta(i\hat{\rho}_2)\hat{\sigma}_1 & (s = +1) \\ \Delta\hat{\rho}_1(i\hat{\sigma}_2) & (s = -1) \end{cases}, \quad (36)$$

where $s = +1(-1)$ represents the odd-band-parity spin-triplet (even-band-parity spin-singlet) pair potential.

The 8×8 BdG Hamiltonian can be block-diagonalized and reduced to two 4×4 Hamiltonians because the normal state Hamiltonian in Eq. (34) does not include any spin-dependent potentials. One of the 4×4 Hamiltonians is given by

$$\check{H}(\mathbf{k}) = \begin{bmatrix} \hat{H}_N & \hat{\Delta} \\ \hat{\Delta}^\dagger & -\hat{H}_N \end{bmatrix}, \quad (37)$$

$$\hat{H}_N = \xi_{\mathbf{k}}\hat{\rho}_0 + \varepsilon\hat{\rho}_3 + V\hat{\rho}_1, \quad (38)$$

$$\hat{\Delta} = \begin{cases} \Delta(i\hat{\rho}_2) & (s = +1) \\ \Delta\hat{\rho}_1 & (s = -1) \end{cases}. \quad (39)$$

We first discuss the results for odd-band-parity spin-triplet SCs ($s = +1$). It has already been reported that the transition to the uniform superconducting phase becomes discontinuous for sufficiently large V or ε [13, 40]. The anomalous Green's function in the reduced subspace for the uniform superconducting state is calculated as [13]

$$\hat{\mathcal{F}}_+(\mathbf{k}, i\omega_\ell) = \frac{-1}{Z_+} [\omega_\ell^2 + \xi_{\mathbf{k}}^2 - \varepsilon^2 - V^2 + \Delta^2 - 2i\omega_\ell(\varepsilon\hat{\rho}_3 + V\hat{\rho}_1)] \Delta(i\hat{\rho}_2), \quad (40)$$

$$Z_+ = \xi_{\mathbf{k}}^4 + 2\xi_{\mathbf{k}}^2 A_+ + C_+ = Z_z|_{h \rightarrow \sqrt{\varepsilon^2 + V^2}}, \quad (41)$$

$$A_+ = \omega_\ell^2 - \varepsilon^2 - V^2 + \Delta^2, \quad (42)$$

$$C_+ = A_+^2 + 4\omega_\ell^2(\varepsilon^2 + V^2). \quad (43)$$

Both the band hybridization V and the band asymmetry ε induce pairing correlations belonging to the odd-frequency symmetry class, as shown in the last term of Eq. (40). The BdG Hamiltonian is equivalent to that of a conventional spin-singlet SC under Zeeman fields in Sec. IV. The GL coefficient and the Meissner kernel have the same structure as those in Eqs. (29), (30) and (31). In the continuum limit, the results are given by

$$a_+(T) = \frac{1}{g} - 2N_0\pi T \sum_{\omega_\ell} \frac{\omega_\ell^2}{|\omega_\ell|(\omega_\ell^2 + \varepsilon^2 + V^2)}, \quad (44)$$

$$K_{+, \mu\nu}(\mathbf{0}, 0) = \delta_{\mu\nu} \frac{4ne^2}{m} Q_+, \quad (45)$$

$$Q_+ = Q_z|_{h \rightarrow \sqrt{\varepsilon^2 + V^2}}, \quad (46)$$

where Q_z is defined in Eq. (31). Therefore, $K_{+, \mu\nu}$ changes sign and becomes negative for sufficiently large $\sqrt{\varepsilon^2 + V^2}$ [13]. In the numerical simulation, we use the same parameters as those in Sec. IV: $\mu = t$, $T_c = 0.05t$, $\Delta_0 = \pi e^{-C} T_c$, and $\mathbf{q} = (q, 0)$. The phase boundary for $s = +1$ can be obtained by replacing the horizontal axis h with $\sqrt{\varepsilon^2 + V^2}$ in Figs. 1(a) and (d).

For even-band-parity spin-singlet SCs with $s = -1$, we

obtain

$$\hat{\mathcal{F}}_-(\mathbf{k}, i\omega_\ell) = \frac{-1}{Z_-} [\omega_\ell^2 + \xi_{\mathbf{k}}^2 - \varepsilon^2 + V^2 + \Delta^2 - 2(\xi_{\mathbf{k}}V\hat{\rho}_1 - i\varepsilon V\hat{\rho}_2 + i\omega_\ell\varepsilon\hat{\rho}_3)] \Delta\hat{\rho}_1, \quad (47)$$

$$Z_- = \xi_{\mathbf{k}}^4 + 2\xi_{\mathbf{k}}^2 A_- + C_-, \quad (48)$$

$$A_- = A_+, \quad (49)$$

$$C_- = A_-^2 + 4(\omega_\ell^2\varepsilon^2 + \omega_\ell^2V^2 + V^2\Delta^2). \quad (50)$$

The band hybridization V induces subdominant even-frequency pairing correlation, whereas the band asymmetry ε induces both even- and odd-frequency pairing correlations. The GL coefficient and the Meissner kernel in the continuum limit are given by

$$a_-(T) = \frac{1}{g} - 2N_0\pi T \sum_{\omega_\ell} \frac{\omega_\ell^2 + V^2}{|\omega_\ell|(\omega_\ell^2 + \varepsilon^2 + V^2)}, \quad (51)$$

$$K_{-, \mu\nu}(\mathbf{0}, 0) = \delta_{\mu\nu} \frac{4ne^2}{m} Q_-, \quad (52)$$

$$Q_- = \sqrt{2}\pi T \sum_{\omega_\ell} \frac{\Delta^2}{[C_-(A_- + \sqrt{C_-})]^{3/2}} \times \left[A_-^3 + \sqrt{C_-}(A_-^2 - 2\omega_\ell^2\varepsilon^2) + 2V^2 \left\{ C_- + 2(\omega_\ell^2 + \Delta^2)(A_- + \sqrt{C_-}) \right\} \right]. \quad (53)$$

While the odd-frequency correlation induced by the band asymmetry ε reduces $K_{-, \mu\nu}$ and eventually changes its sign to negative, the even-frequency correlation induced by the hybridization V enhances the Meissner kernel. Thus, finite-momentum superconducting states are expected for sufficiently large ε . To confirm this, we numerically solve $[D_s^R(\mathbf{q}, 0)]^{-1} = 0$ on the tight-binding model. The parameters in the numerical simulation are the same as those in Sec. IV: $\mu = t$, $T_c = 0.05t$, $\Delta_0 = \pi e^{-C}T_c$, and $\mathbf{q} = (q, 0)$. The results for $V = 0.3\Delta_0$ are shown in Fig. 1(b). The magnitude of \mathbf{q} at the transition point is also plotted as a function of ε in (e). The transition to the finite-momentum superconducting state occurs for $\varepsilon \gtrsim 0.6\Delta_0$, as indicated by red dots in (b) and (e). The characteristic features in (b) and (e) are essentially the same as those in (a) and (d). The resulting q are much smaller than $k_F \sim 1/c_0$, which justifies the expansion in Eq. (17).

B. $j = 3/2$ SC with a pseudospin-quintet pairing order

An electron in a $j = 3/2$ SC is characterized by a total angular momentum $j = 3/2$, resulting from strong coupling between spin $s = 1/2$ and orbital angular momentum $\ell = 1$ [41]. The s -wave pseudospin-quintet pair potential represents a superconducting state due to the Cooper pairing between two such high-pseudospin electrons. To describe the electronic structure on a simple

cubic lattice, we choose

$$\hat{\xi}_{\mathbf{k}} = \xi_{\mathbf{k}} 1_{4 \times 4} + \vec{\epsilon}_{\mathbf{k}} \cdot \vec{\gamma}, \quad \hat{w}(\mathbf{k}) = \frac{1}{\sqrt{2}} \gamma^4 U_T, \quad (54)$$

$$\xi_{\mathbf{k}} = \left(-2t_1 - \frac{5}{2}t_2 \right) \sum_{\nu} \cos k_{\nu} + 6t_1 + \frac{15}{2}t_2 - \mu, \quad (55)$$

$$\epsilon_{\mathbf{k},1} = 4\sqrt{3}t_3 \sin k_x \sin k_y, \quad (56)$$

$$\epsilon_{\mathbf{k},2} = 4\sqrt{3}t_3 \sin k_y \sin k_z, \quad (57)$$

$$\epsilon_{\mathbf{k},3} = 4\sqrt{3}t_3 \sin k_z \sin k_x, \quad (58)$$

$$\epsilon_{\mathbf{k},4} = \sqrt{3}t_2 (-\cos k_x + \cos k_y), \quad (59)$$

$$\epsilon_{\mathbf{k},5} = t_2 (-2 \cos k_z + \cos k_x + \cos k_y), \quad (60)$$

$$U_T = \gamma^1 \gamma^2, \quad (61)$$

in Eq. (9) [41, 82–86], where the definitions of the five 4×4 matrices γ^j for $j = 1 - 5$ and their algebra are shown in Appendix C. The length is measured in units of the lattice constant $c_0 = 1$. The dispersion $\xi_{\mathbf{k}}$ is independent of the pseudospin of an electron, whereas that of the five-component vector $\vec{\epsilon}_{\mathbf{k}} = (\epsilon_{\mathbf{k},1}, \epsilon_{\mathbf{k},2}, \epsilon_{\mathbf{k},3}, \epsilon_{\mathbf{k},4}, \epsilon_{\mathbf{k},5})$ depends on pseudospin. The pair potential is given by $\hat{\Delta}(\mathbf{k}) = \Delta \gamma^4 U_T$. Although we set $t_2 = 0$ for simplicity, we retain $t_3 \ll t_1$ as a source of odd-frequency pairing correlations. The anomalous Green's function for the uniform superconducting state is given by [13]

$$\hat{\mathcal{F}}_{3/2}(\mathbf{k}, i\omega_\ell) = -\frac{\Delta}{Z_{3/2}} [W - 2i\omega_\ell \vec{\epsilon}_{\mathbf{k}} \cdot \vec{\gamma}] \gamma^4 U_T, \quad (62)$$

$$Z_{3/2} = W^2 + 4\omega_\ell^2 \vec{\epsilon}_{\mathbf{k}}^2, \quad W = \omega_\ell^2 + \xi_{\mathbf{k}}^2 - \vec{\epsilon}_{\mathbf{k}}^2 + \Delta^2. \quad (63)$$

The spin-orbit interaction $\vec{\epsilon}_{\mathbf{k}}$ induces a subdominant odd-frequency pairing correlation, as shown in the second term in Eq. (62) [13]. The GL coefficient and the contribution of the anomalous Green's function to the Meissner kernel, $K^{\mathcal{F}}$, in the lattice model are given by [13, 87, 88]

$$a_{3/2}(T) = \frac{1}{g} - 2T \sum_{\omega_\ell} \frac{1}{N} \sum_{\mathbf{k}} \frac{1}{Z_{3/2}|_{\Delta=0}} (\omega_\ell^2 + \xi_{\mathbf{k}}^2 - \vec{\epsilon}_{\mathbf{k}}^2), \quad (64)$$

$$K_{3/2,xx}^{\mathcal{F}}(\mathbf{0}, 0) = 16e^2 T \sum_{\omega_\ell} \frac{1}{N} \sum_{\mathbf{k}} t_1^2 \sin^2 k_x \frac{\Delta^2}{Z_{3/2}^2} [W^2 - 4\omega_\ell^2 \vec{\epsilon}_{\mathbf{k}}^2], \quad (65)$$

where, for simplicity, we neglect the correction to the velocity operator arising from the weak spin-orbit interaction ($t_3 \ll t_1$) [13]. The second term in Eq. (65) represents the negative contribution of odd-frequency correlations to the Meissner kernel. Therefore, finite-momentum superconducting states can be expected when the amplitude of the spin-orbit interaction t_3 is sufficiently large. Figures 1(c) and (f) show the numerical solutions of $[D_s^R(\mathbf{q}, 0)]^{-1} = 0$, where we choose $\mu = t_1$, $t_2 = 0$, $T_c = 0.05t_1$, $\Delta_0 = \pi e^{-C}T_c$, and $\mathbf{q} = (q, 0, 0)$. The characteristic features in (c) and (f) are qualitatively the same as those in (a) and (d). The resulting q are much smaller than $k_F \sim 1/c_0$, which justifies the expansion in Eq. (17).

VI. DISCUSSION

A. Platforms for finite-momentum superconductivity

In Sec. V, we demonstrate the emergence of finite-momentum superconductivity in TRS-preserving SCs. Here, we briefly discuss the possibility in real materials. In the present analysis, we focus only on interband/orbital superconductivity, in which electrons belonging to different bands or orbitals experience attractive interactions, and do not consider intraband/orbital superconductivity, such as that in MgB₂ [89, 90] or iron-based compounds [91, 92]. This is because the magnitudes of odd-frequency pairing correlations in such intraband/orbital SCs tend to be small [93]. Thus, the instability of the uniform state is not expected.

Doped topological insulator Cu_xBi₂Se₃ and related compounds [94, 95] can be representative examples of interband/orbital SCs. In addition, topological superconductivity proposed in bilayer Rashba systems [96] provides another platform for realizing such pairing states. Although the emergence of odd-frequency pairing correlations in Cu_xBi₂Se₃ has been discussed [97, 98], finite-momentum superconducting states have not been reported. Another example is transition-metal dichalcogenide (TMD) SCs, where two valleys located at K and K' points in the Brillouin zone correspond to an extra internal degree of freedom of an electron [99–101]. The pair potential for the Kramers partner is described as an intervalley pair potential. The Hamiltonian of a $j = 3/2$ SC [41] can capture the low-energy electronic structure of a wide class of two-band/orbital SCs, including the above interband/orbital superconducting systems [102]. Therefore, TRS-preserving finite-momentum superconducting states may be realized in these materials.

B. Relation to the discontinuous transition to a uniform state

It is known that the following relation holds between two transition temperatures of a conventional SC in Zeeman fields [44].

$$T_{\text{dis}} = T_{\text{FFLO}}, \quad (66)$$

where T_{FFLO} is the highest second-order transition temperature to the finite-momentum state in the h - T phase diagram, and T_{dis} is the highest first-order (discontinuous) transition temperature to the uniform superconducting state [47, 48]. The reason for the coincidence is well explained by the relations among the superfluid weight $Q(T)$, the quartic coefficient $b(T)$ in the GL free energy for a uniform SC in Eq. (21), and the coefficient $B(T)$ in Eq. (17). This study shows that the relation

$$B(T) = A_B Q(T)/|\Delta|^2|_{\Delta \rightarrow 0}, \quad (67)$$

holds with a constant $A_B > 0$, and that T_{FFLO} is well characterized by $B = Q = 0$. In a previous study [13], we also found that the relation

$$b(T) \approx A_b Q(T)/|\Delta|^2|_{\Delta \rightarrow 0}, \quad (68)$$

is satisfied near the transition temperature for uniform SCs, with $A_b > 0$ being a constant, and that T_{dis} is characterized by $b = Q = 0$ [103]. In such cases, the sign change of the superfluid weight Q characterizes both T_{dis} and T_{FFLO} simultaneously, thereby explaining their coincidence. Equation (66) holds as long as the relation in Eq. (68) is satisfied and the higher order terms in Eq. (17) are negligible [104]. It should be noted that the relation between the sign of the superfluid density and the stability of finite-momentum superconducting states was also implicit in a previous study [105].

VII. CONCLUSION

We have discussed the mechanisms for the emergence of inhomogeneous superconductivity characterized by a small center-of-mass momentum q of Cooper pairs. The analytic expression for the pair fluctuation propagator provides the conditions for the appearance of such finite-momentum superconductivity. When the superfluid density expected in the uniform superconducting state is negative, a finite-momentum superconducting state appears below the transition temperature. The analytic expressions for the superfluid density indicate that the odd-frequency Cooper pairing correlations reduce the superfluid density in a conventional SC in Zeeman fields, two-band SCs with interband pairing order, and a $j = 3/2$ SC. Time-reversal symmetry is preserved in the latter two cases. In all cases, we demonstrate the transition to finite-momentum superconducting states using both the analytic expression for the pair fluctuation propagator and numerical calculations. We conclude that the instability of the uniform superconducting state due to odd-frequency pairing correlations is a source of the emergence of finite-momentum superconducting states.

We have developed a theoretical framework that explains the emergence of finite-momentum superconducting states by considering the negative superfluid density induced by odd-frequency pairing correlations. Our theory provides a unified understanding of inhomogeneous superconducting states in bulk [1, 2, 11, 12] and around local defects [16–23].

ACKNOWLEDGMENTS

T. S. is grateful to S. Ikegaya and K. Aoyama for useful discussions. S. K. was supported by JSPS KAKENHI (Grants No. JP19K14612 and No. JP22K03478) and JST CREST (Grant No. JPMJCR19T2). S. H. was supported by JSPS KAKENHI (Grants No. JP21H01037

and No. JP23H04869) and JST FOREST (Grant No. JPMJFR2366). Y. A. was supported by a Grant-in-Aid for Scientific Research (JSPS KAKENHI Grant No. JP26K0692).

Appendix A: Meissner kernel up to Δ^2

To discuss the linear response of a uniform SC described by \mathcal{H} in Eq. (9) to an external magnetic field, we express the noninteracting Hamiltonian in Eq. (10) in real space:

$$\mathcal{H}_0 = \sum_{\mathbf{r}\mathbf{R}\alpha\beta} \left(-t_{\mathbf{R}}^{\alpha\beta} - \mu\delta_{\mathbf{R},\mathbf{0}}\delta_{\alpha\beta} \right) c_{\mathbf{r}+\mathbf{R}\alpha}^\dagger c_{\mathbf{r}\beta}. \quad (\text{A1})$$

The matrix element of the noninteracting Hamiltonian in momentum space is given by $\epsilon_{\mathbf{k}\alpha\beta} = \sum_{\mathbf{R}} -t_{\mathbf{R}}^{\alpha\beta} e^{-i\mathbf{k}\cdot\mathbf{R}}$. The coupling between electrons and an electromagnetic field is introduced through the Peierls phase in the hopping $t_{\mathbf{R}}^{\alpha\beta}$ in \mathcal{H}_0 [106, 107]:

$$-t_{\mathbf{R}}^{\alpha\beta} \rightarrow -t_{\mathbf{R}}^{\alpha\beta} e^{i\varphi_{\mathbf{R}}(\mathbf{r})}, \quad (\text{A2})$$

$$\varphi_{\mathbf{R}}(\mathbf{r}) = e \int_{\mathbf{r}}^{\mathbf{r}+\mathbf{R}} d\mathbf{r}' \cdot \mathbf{A}(\mathbf{r}') \approx e\mathbf{A}(\mathbf{r} + \mathbf{R}/2) \cdot \mathbf{R}, \quad (\text{A3})$$

where the approximation in Eq. (A3) is justified when the vector potential varies on a length scale much larger than the lattice spacing. We also assume that the Peierls phase is independent of the internal degrees of freedom of an electron and that the vector potential does not couple to the effective electron-electron interaction Hamiltonian \mathcal{H}_1 . The current density operator is defined via the variation of the Hamiltonian with respect to the vector potential:

$$\delta\mathcal{H}_A = \mathcal{H}_{A+\delta A} - \mathcal{H}_A = - \sum_{\ell} \mathbf{j}_{\ell} \cdot \delta\mathbf{A}_{\ell} + O(\delta A^2), \quad (\text{A4})$$

where \mathcal{H}_A is the total Hamiltonian including the Peierls phase. The current density operator is then given by

$$\mathbf{j}_{\ell}(t) := \sum_{\substack{\mathbf{r}\mathbf{R} \\ \alpha\beta}} ie\mathbf{R} t_{\mathbf{R}}^{\alpha\beta} e^{ie\mathbf{A}_{\ell}\cdot\mathbf{R}} c_{\mathbf{r}+\mathbf{R}\alpha}^\dagger c_{\mathbf{r}\beta} \delta_{\ell,\mathbf{r}+\mathbf{R}/2}. \quad (\text{A5})$$

To first order in the vector potential, the current density operator can be decomposed into paramagnetic and diamagnetic contributions:

$$j_{\mu\ell}(t) = j_{\mu\ell}^{\text{para}} + j_{\mu\ell}^{\text{dia}}(t) + O(A^2), \quad (\text{A6})$$

$$j_{\mu\ell}^{\text{para}} := ie \sum_{\substack{\mathbf{r}\mathbf{R} \\ \alpha\beta}} R_{\mu} t_{\mathbf{R}}^{\alpha\beta} c_{\mathbf{r}+\mathbf{R}\alpha}^\dagger c_{\mathbf{r}\beta} \delta_{\ell,\mathbf{r}+\mathbf{R}/2}, \quad (\text{A7})$$

$$j_{\mu\ell}^{\text{dia}}(t) := -e^2 \sum_{\substack{\mathbf{r}\mathbf{R} \\ \alpha\beta}} R_{\mu} R_{\nu} t_{\mathbf{R}}^{\alpha\beta} c_{\mathbf{r}+\mathbf{R}\alpha}^\dagger c_{\mathbf{r}\beta} A_{\nu\ell}(t) \delta_{\ell,\mathbf{r}+\mathbf{R}/2}. \quad (\text{A8})$$

The total Hamiltonian in the presence of a vector potential reads

$$\mathcal{H}_A = \mathcal{H} - \sum_{\ell} \mathbf{j}_{\ell}^{\text{para}} \cdot \mathbf{A}_{\ell}(t) + O(A^2). \quad (\text{A9})$$

We consider only transverse gauge fields (i.e., $\mathbf{q} \cdot \mathbf{A}_{\mathbf{q}} = 0$). The expectation value of the current density is calculated using linear response theory [108–110]:

$$\begin{aligned} \langle j_{\mu\mathbf{q}} \rangle(\omega) &= -K_{\mu\nu}(\mathbf{q}, \omega) A_{\nu\mathbf{q}}(\omega) \\ &= \langle j_{\mu\mathbf{q}} \rangle(\omega) + \Lambda_{\mu\nu}^{\text{R}}(\mathbf{q}, \omega) A_{\nu\mathbf{q}}(\omega), \end{aligned} \quad (\text{A10})$$

where $\langle j_{\mu\mathbf{q}} \rangle(\omega)$ and $\Lambda_{\mu\nu}^{\text{R}}(\mathbf{q}, \omega)$ are the Fourier components of the expectation value of the current density operator and the current-current correlation function, respectively. Within the mean-field approximation, they are calculated as follows:

$$\langle j_{\mu\mathbf{q}} \rangle(\omega) = -e^2 T \sum_{\omega_{\ell}} \frac{1}{N} \sum_{\mathbf{k}} \text{Tr} \left[\partial_{k_{\mu}} \partial_{k_{\nu}} \hat{\epsilon}_{\mathbf{k}} \hat{\mathcal{G}}(\mathbf{k}, i\omega_{\ell}) \right] e^{i\omega_{\ell}\eta} A_{\nu\mathbf{q}}(\omega), \quad (\text{A11})$$

$$\Lambda_{\mu\nu}^{\text{R}}(\mathbf{q}, \omega) = \Lambda_{\mu\nu}(\mathbf{q}, i\nu_n \rightarrow \omega + i\delta), \quad (\text{A12})$$

$$\Lambda_{\mu\nu}(\mathbf{q}, i\nu_n) = \int_0^{\beta} d\tau \frac{1}{N} \langle T_{\tau} j_{\mu\mathbf{q}}^{\text{para}}(\tau) j_{\nu-\mathbf{q}}^{\text{para}} \rangle e^{i\nu_n\tau} \quad (\text{A13})$$

$$\begin{aligned} &= -e^2 T \sum_{\omega_{\ell}} \frac{1}{N} \sum_{\mathbf{k}} \text{Tr} \left[\hat{v}_{\mu}(\mathbf{k} + \mathbf{q}/2) \hat{\mathcal{G}}(\mathbf{k} + \mathbf{q}, i\omega_{\ell} + i\nu_n) \hat{v}_{\nu}(\mathbf{k} + \mathbf{q}/2) \hat{\mathcal{G}}(\mathbf{k}, i\omega_{\ell}) \right. \\ &\quad \left. + \hat{v}_{\mu}(\mathbf{k} + \mathbf{q}/2) \hat{\mathcal{F}}(\mathbf{k} + \mathbf{q}, i\omega_{\ell} + i\nu_n) \hat{\underline{v}}_{\nu}(\mathbf{k} + \mathbf{q}/2) \hat{\underline{\mathcal{F}}}(\mathbf{k}, i\omega_{\ell}) \right], \end{aligned} \quad (\text{A14})$$

where we assumed $\langle j_{\mu\mathbf{q}}^{\text{para}} \rangle = 0$, η and δ are small positive real values, and $\mathcal{G}(\mathcal{F})$ is the normal (anomalous) Green's function. The mean-field Hamiltonian and the Green's functions are given by

$$\mathcal{H}^{\text{MF}} = \mathcal{H}_0 + \mathcal{H}_1^{\text{MF}} = \frac{1}{2} \sum_{\mathbf{k}} \vec{\Psi}_{\mathbf{k}}^\dagger H(\mathbf{k}) \vec{\Psi}_{\mathbf{k}} + \text{const.}, \quad (\text{A15})$$

$$H(\mathbf{k}) = \begin{bmatrix} \hat{\xi}_{\mathbf{k}} & \hat{\Delta}(\mathbf{k}) \\ -\hat{\Delta}^*(-\mathbf{k}) & -\hat{\xi}_{-\mathbf{k}}^* \end{bmatrix}, \quad \vec{\Psi}_{\mathbf{k}} = [\vec{\psi}_{\mathbf{k}}^T, \vec{\psi}_{-\mathbf{k}}^\dagger]^T, \quad \vec{\psi}_{\mathbf{k}} = [c_{\mathbf{k}1}, c_{\mathbf{k}2}, \dots, c_{\mathbf{k}M}]^T, \quad (\text{A16})$$

$$\begin{bmatrix} \hat{\mathcal{G}} & \hat{\mathcal{F}} \\ \hat{\mathcal{F}} & \hat{\mathcal{G}} \end{bmatrix}_{(\mathbf{k}, i\omega_\ell)} = [i\omega_\ell - H(\mathbf{k})]^{-1}, \quad (\text{A17})$$

where M is the number of internal degrees of freedom of the electron, $H(\mathbf{k})$ is a $2M \times 2M$ matrix, and the mean field is defined as follows:

$$\Delta_{\sigma\sigma'}(\mathbf{k}) := w_{\sigma\sigma'}(\mathbf{k}) \sum_{\gamma\delta} \frac{g}{N} \sum_{\mathbf{k}'} w_{\gamma\delta}^*(\mathbf{k}') \langle c_{\mathbf{k}'\gamma} c_{-\mathbf{k}'\delta} \rangle. \quad (\text{A18})$$

The response to a static, uniform magnetic field is described by $K_{\mu\nu}(\mathbf{q} \rightarrow \mathbf{0}, \omega = 0)$. We obtain

$$K_{\mu\nu}(\mathbf{0}, 0) = e^2 T \sum_{\omega_\ell} \frac{1}{N} \sum_{\mathbf{k}} \text{Tr} \left[\partial_{k_\mu} \partial_{k_\nu} \hat{\epsilon}_{\mathbf{k}} \hat{\mathcal{G}}(\mathbf{k}, i\omega_\ell) e^{i\omega_\ell \eta} \right. \\ \left. + \hat{v}_\mu(\mathbf{k}) \hat{\mathcal{G}}(\mathbf{k}, i\omega_\ell) \hat{v}_\nu(\mathbf{k}) \hat{\mathcal{G}}(\mathbf{k}, i\omega_\ell) + \hat{v}_\mu(\mathbf{k}) \hat{\mathcal{F}}(\mathbf{k}, i\omega_\ell) \hat{\mathcal{G}}(\mathbf{k}, i\omega_\ell) \right]. \quad (\text{A19})$$

The contribution from the anomalous Green's function is defined as

$$K_{\mu\nu}^{\mathcal{F}}(\mathbf{0}, 0) := e^2 T \sum_{\omega_\ell} \frac{1}{N} \sum_{\mathbf{k}} \text{Tr} \left[\hat{v}_\mu(\mathbf{k}) \hat{\mathcal{F}}(\mathbf{k}, i\omega_\ell) \hat{\mathcal{G}}(\mathbf{k}, i\omega_\ell) \right], \quad (\text{A20})$$

in Eq. (65). Expanding the Green's function with respect to Δ , we obtain

$$K_{\mu\nu}(\mathbf{0}, 0) = e^2 T \sum_{\omega_\ell} \frac{1}{N} \sum_{\mathbf{k}} \text{Tr} \left[\partial_{k_\mu} \partial_{k_\nu} \hat{\epsilon}_{\mathbf{k}} \hat{\mathcal{G}}_0 \hat{\Delta} \hat{\mathcal{G}}_0 \hat{\Delta} \hat{\mathcal{G}}_0 e^{i\omega_\ell \eta} + \hat{v}_\mu \hat{\mathcal{G}}_0 \hat{v}_\nu \hat{\mathcal{G}}_0 \hat{\Delta} \hat{\mathcal{G}}_0 \hat{\Delta} \hat{\mathcal{G}}_0 \right. \\ \left. + \hat{v}_\mu \hat{\mathcal{G}}_0 \hat{\Delta} \hat{\mathcal{G}}_0 \hat{\Delta} \hat{\mathcal{G}}_0 \hat{v}_\nu \hat{\mathcal{G}}_0 + \hat{v}_\mu \hat{\mathcal{G}}_0 \hat{\Delta} \hat{\mathcal{G}}_0 \hat{v}_\nu \hat{\mathcal{G}}_0 \hat{\Delta} \hat{\mathcal{G}}_0 \right] + O(\Delta^4), \quad (\text{A21})$$

where we assume the absence of the Meissner effect in the normal state:

$$K_{\mu\nu}^{\text{N}}(\mathbf{0}, 0) := e^2 T \sum_{\omega_\ell} \frac{1}{N} \sum_{\mathbf{k}} \text{Tr} \left[\partial_{k_\mu} \partial_{k_\nu} \hat{\epsilon}_{\mathbf{k}} \hat{\mathcal{G}}_0 e^{i\omega_\ell \eta} + \hat{v}_\mu \hat{\mathcal{G}}_0 \hat{v}_\nu \hat{\mathcal{G}}_0 \right] = 0. \quad (\text{A22})$$

Appendix B: Normal Green's function

The normal Green's functions in the uniform superconducting states of the three theoretical models are summarized in this section. The result for a conventional SC under a Zeeman field discussed in Sec. IV reads as follows:

$$\hat{\mathcal{G}}_z(\mathbf{k}, i\omega_\ell) = \frac{-1}{Z_z} [(i\omega_\ell + \xi_{\mathbf{k}})(\omega_\ell^2 + \xi_{\mathbf{k}}^2 + \Delta^2) + (i\omega_\ell - \xi_{\mathbf{k}})h^2] \\ + \{(i\omega_\ell + \xi_{\mathbf{k}})^2 - h^2 + \Delta^2\} \mathbf{h} \cdot \hat{\boldsymbol{\sigma}}. \quad (\text{B1})$$

The result for a two-band SC with $s = +1$ discussed

in Sec. V A is given by

$$\hat{\mathcal{G}}_+(\mathbf{k}, i\omega_\ell) = \frac{-1}{Z_+} [(i\omega_\ell + \xi_{\mathbf{k}})(\omega_\ell^2 + \xi_{\mathbf{k}}^2 + \Delta^2) + (i\omega_\ell - \xi_{\mathbf{k}})(\varepsilon^2 + V^2)] \\ - \{(i\omega_\ell + \xi_{\mathbf{k}})^2 - (\varepsilon^2 + V^2) + \Delta^2\} (\varepsilon \hat{\rho}_3 + V \hat{\rho}_1). \quad (\text{B2})$$

For $s = -1$, we obtain

$$\hat{\mathcal{G}}_-(\mathbf{k}, i\omega_\ell) = \frac{-1}{Z_-} [(i\omega_\ell + \xi_{\mathbf{k}})(\omega_\ell^2 + \xi_{\mathbf{k}}^2 + \Delta^2) + (i\omega_\ell - \xi_{\mathbf{k}})(\varepsilon^2 + V^2)] \\ - \{(i\omega_\ell + \xi_{\mathbf{k}})^2 - (\varepsilon^2 + V^2) + \Delta^2\} (\varepsilon \hat{\rho}_3 + V \hat{\rho}_1) \\ + 2V \Delta^2 \hat{\rho}_1. \quad (\text{B3})$$

In the $j = 3/2$ SC discussed in Sec. VB with $t_2 = 0$, we obtain

Appendix C: Algebras of γ matrices

The angular momentum operators for $j = 3/2$ electrons are given by

$$J_x = \frac{1}{2} \begin{bmatrix} 0 & \sqrt{3} & 0 & 0 \\ \sqrt{3} & 0 & 2 & 0 \\ 0 & 2 & 0 & \sqrt{3} \\ 0 & 0 & \sqrt{3} & 0 \end{bmatrix}, \quad (C1)$$

$$J_y = \frac{1}{2} \begin{bmatrix} 0 & -i\sqrt{3} & 0 & 0 \\ i\sqrt{3} & 0 & -2i & 0 \\ 0 & 2i & 0 & -i\sqrt{3} \\ 0 & 0 & i\sqrt{3} & 0 \end{bmatrix}, \quad (C2)$$

$$J_z = \frac{1}{2} \begin{bmatrix} 3 & 0 & 0 & 0 \\ 0 & 1 & 0 & 0 \\ 0 & 0 & -1 & 0 \\ 0 & 0 & 0 & -3 \end{bmatrix}. \quad (C3)$$

The five Dirac's γ -matrices are defined in the 4×4 pseudospin space as

$$\gamma^1 = \frac{1}{\sqrt{3}}(J_x J_y + J_y J_x), \quad \gamma^2 = \frac{1}{\sqrt{3}}(J_y J_z + J_z J_y), \quad (C4)$$

$$\gamma^3 = \frac{1}{\sqrt{3}}(J_z J_x + J_x J_z), \quad \gamma^4 = \frac{1}{\sqrt{3}}(J_x^2 - J_y^2), \quad (C5)$$

$$\gamma^5 = \frac{1}{3}(2J_z^2 - J_x^2 - J_y^2), \quad (C6)$$

and $1_{4 \times 4}$ denotes the identity matrix. They satisfy the following relations:

$$\gamma^i \gamma^j + \gamma^j \gamma^i = 2 \times 1_{4 \times 4} \delta_{i,j}, \quad (C7)$$

$$\gamma^1 \gamma^2 \gamma^3 \gamma^4 \gamma^5 = -1_{4 \times 4}, \quad (C8)$$

$$\{\gamma^i\}^* = \{\gamma^i\}^T = U_T \gamma^i U_T^{-1}, \quad U_T = \gamma^1 \gamma^2, \quad (C9)$$

where U_T is the unitary part of the time-reversal operator $\mathcal{T} = U_T \mathcal{K}$, with \mathcal{K} denoting complex conjugation.

$$\begin{aligned} \hat{\mathcal{G}}_{3/2}(\mathbf{k}, i\omega_n) = & \\ \frac{-1}{Z_{3/2}} & [(i\omega_n + \xi_{\mathbf{k}})(\omega_n^2 + \xi_{\mathbf{k}}^2 + \Delta^2) + (i\omega_n - \xi_{\mathbf{k}})\bar{\epsilon}_{\mathbf{k}}^2 \\ & - \{(i\omega_n + \xi_{\mathbf{k}})^2 - \bar{\epsilon}_{\mathbf{k}}^2 + \Delta^2\} \bar{\epsilon}_{\mathbf{k}} \cdot \vec{\gamma}]. \end{aligned} \quad (B4)$$

-
- [1] P. Fulde and R. A. Ferrell, Superconductivity in a Strong Spin-Exchange Field, *Phys. Rev.* **135**, A550 (1964).
- [2] A. I. Larkin and Y. N. Ovchinnikov, Nonuniform state of superconductors, *Zh. Eksp. Teor. Fiz.* **47**, 1136 (1964), [*Sov. Phys. JETP* **20**, 762 (1965)].
- [3] S. Sumita, M. Naka, and H. Seo, Fulde-Ferrell-Larkin-Ovchinnikov state induced by antiferromagnetic order in κ -type organic conductors, *Phys. Rev. Res.* **5**, 043171 (2023).
- [4] S.-B. Zhang, L.-H. Hu, and T. Neupert, Finite-momentum Cooper pairing in proximitized altermagnets, *Nature Communications* **15**, 1801 (2024).
- [5] D. Chakraborty and A. M. Black-Schaffer, Zero-field finite-momentum and field-induced superconductivity in altermagnets, *Phys. Rev. B* **110**, L060508 (2024).
- [6] N. F. Q. Yuan and L. Fu, Supercurrent diode effect and finite-momentum superconductors, *Proceedings of the National Academy of Sciences* **119**, e2119548119, <https://www.pnas.org/doi/pdf/10.1073/pnas.2119548119>.
- [7] A. Daido, Y. Ikeda, and Y. Yanase, Intrinsic Superconducting Diode Effect, *Phys. Rev. Lett.* **128**, 037001 (2022).
- [8] J. J. He, Y. Tanaka, and N. Nagaosa, A phenomenological theory of superconductor diodes, *New Journal of Physics* **24**, 053014 (2022).
- [9] J. Hasan, D. Shaffer, M. Khodas, and A. Levchenko, Supercurrent diode effect in helical superconductors, *Phys. Rev. B* **110**, 024508 (2024).
- [10] D. Shaffer, D. V. Chichinadze, and A. Levchenko, Supercurrent diode effect in multiphase superconductors, *Phys. Rev. B* **110**, 184509 (2024).

- [11] V. P. Mineev and K. V. Samokhin, Nonuniform states in noncentrosymmetric superconductors: Derivation of Lifshitz invariants from microscopic theory, *Phys. Rev. B* **78**, 144503 (2008).
- [12] G. Li and P. M. R. Brydon, Collective modes in an unconventional superconductor with $j = \frac{3}{2}$ fermions, *Phys. Rev. B* **110**, 144501 (2024).
- [13] T. Sato, S. Kobayashi, and Y. Asano, Discontinuous transition to a superconducting phase, *Phys. Rev. B* **110**, 144503 (2024).
- [14] D. F. Agterberg, J. S. Davis, S. D. Edkins, E. Fradkin, D. J. Van Harlingen, S. A. Kivelson, P. A. Lee, L. Radzihovsky, J. M. Tranquada, and Y. Wang, The Physics of Pair-Density Waves: Cuprate Superconductors and Beyond, *Annual Review of Condensed Matter Physics* **11**, 231 (2020).
- [15] D. Chakraborty and A. M. Black-Schaffer, Odd-frequency pair density wave correlations in underdoped cuprates, *New Journal of Physics* **23**, 033001 (2021).
- [16] Y. Tanuma, N. Hayashi, Y. Tanaka, and A. A. Golubov, Model for Vortex-Core Tunneling Spectroscopy of Chiral p -Wave Superconductors via Odd-Frequency Pairing States, *Phys. Rev. Lett.* **102**, 117003 (2009).
- [17] D. Kuzmanovski, R. S. Souto, and A. V. Balatsky, Odd-frequency superconductivity near a magnetic impurity in a conventional superconductor, *Phys. Rev. B* **101**, 094505 (2020).
- [18] V. Perrin, F. L. N. Santos, G. C. Ménard, C. Brun, T. Cren, M. Civelli, and P. Simon, Unveiling Odd-Frequency Pairing around a Magnetic Impurity in a Superconductor, *Phys. Rev. Lett.* **125**, 117003 (2020).
- [19] S.-I. Suzuki, T. Sato, and Y. Asano, Odd-frequency Cooper pair around a magnetic impurity, *Phys. Rev. B* **106**, 104518 (2022).
- [20] S.-I. Suzuki, T. Sato, and Y. Asano, π -phase Shift of the Pair Potential under a Magnetic Cluster, *JPS Conf. Proc.* **38**, 011067 (2023), <https://journals.jps.jp/doi/pdf/10.7566/JPSCP.38.011067>.
- [21] S.-I. Suzuki, T. Sato, A. A. Golubov, and Y. Asano, Fulde-Ferrell-Larkin-Ovchinnikov state in a superconducting thin film attached to a ferromagnetic cluster, *Phys. Rev. B* **108**, 064509 (2023).
- [22] Y. Tanaka and A. A. Golubov, Theory of the Proximity Effect in Junctions with Unconventional Superconductors, *Phys. Rev. Lett.* **98**, 037003 (2007).
- [23] Y. Asano and Y. Tanaka, Majorana fermions and odd-frequency Cooper pairs in a normal-metal nanowire proximity-coupled to a topological superconductor, *Phys. Rev. B* **87**, 104513 (2013).
- [24] V. L. Berezinskii, New model of the anisotropic phase of superfluid He³, *Pis'ma Zh. Eksp. Teor. Fiz.* **20**, 628 (1974), [*JETP Lett.* **20**, 287 (1974)].
- [25] F. S. Bergeret, A. F. Volkov, and K. B. Efetov, Odd triplet superconductivity and related phenomena in superconductor-ferromagnet structures, *Rev. Mod. Phys.* **77**, 1321 (2005).
- [26] Y. Tanaka, M. Sato, and N. Nagaosa, Symmetry and Topology in Superconductors - Odd-Frequency Pairing and Edge States-, *Journal of the Physical Society of Japan* **81**, 011013 (2012).
- [27] J. Linder and A. V. Balatsky, Odd-frequency superconductivity, *Rev. Mod. Phys.* **91**, 045005 (2019).
- [28] C. Triola, J. Cayao, and A. M. Black-Schaffer, The Role of Odd-Frequency Pairing in Multiband Superconductors, *Annalen der Physik* **532**, 1900298 (2020), <https://onlinelibrary.wiley.com/doi/pdf/10.1002/andp.201900298>.
- [29] J. Cayao, C. Triola, and A. M. Black-Schaffer, Odd-frequency superconducting pairing in one-dimensional systems, *The European Physical Journal Special Topics* **229**, 545 (2020).
- [30] Y. Asano, Y. V. Fominov, and Y. Tanaka, Consequences of bulk odd-frequency superconducting states for the classification of Cooper pairs, *Phys. Rev. B* **90**, 094512 (2014).
- [31] Y. Asano, A. A. Golubov, Y. V. Fominov, and Y. Tanaka, Unconventional Surface Impedance of a Normal-Metal Film Covering a Spin-Triplet Superconductor Due to Odd-Frequency Cooper Pairs, *Phys. Rev. Lett.* **107**, 087001 (2011).
- [32] S.-I. Suzuki and Y. Asano, Paramagnetic instability of small topological superconductors, *Phys. Rev. B* **89**, 184508 (2014).
- [33] S. Higashitani, Odd-frequency pairing effect on the superfluid density and the Pauli spin susceptibility in spatially nonuniform spin-singlet superconductors, *Phys. Rev. B* **89**, 184505 (2014).
- [34] A. M. Black-Schaffer and A. V. Balatsky, Odd-frequency superconducting pairing in multiband superconductors, *Phys. Rev. B* **88**, 104514 (2013).
- [35] Y. Asano and A. Sasaki, Odd-frequency Cooper pairs in two-band superconductors and their magnetic response, *Phys. Rev. B* **92**, 224508 (2015).
- [36] K. V. Samokhin and B. P. Truong, Current-carrying states in Fulde-Ferrell-Larkin-Ovchinnikov superconductors, *Phys. Rev. B* **96**, 214501 (2017).
- [37] T. Kitamura, A. Daido, and Y. Yanase, Quantum geometric effect on Fulde-Ferrell-Larkin-Ovchinnikov superconductivity, *Phys. Rev. B* **106**, 184507 (2022).
- [38] L. N. Cooper, Bound Electron Pairs in a Degenerate Fermi Gas, *Phys. Rev.* **104**, 1189 (1956).
- [39] V. Ambegaokar, *Superconductivity*, edited by R. D. Parks, Vol. 1 (Marcel Dekker, 1969) p. 259.
- [40] M. Gomes da Silva, F. Dinóla Neto, I. Padilha, J. Ricardo de Sousa, and M. Continentino, First-order superconducting transition in the inter-band model, *Physics Letters A* **378**, 1396 (2014).
- [41] P. M. R. Brydon, L. Wang, M. Weinert, and D. F. Agterberg, Pairing of $j = 3/2$ Fermions in Half-Heusler Superconductors, *Phys. Rev. Lett.* **116**, 177001 (2016).
- [42] B. S. Chandrasekhar, A NOTE ON THE MAXIMUM CRITICAL FIELD OF HIGH-FIELD SUPERCONDUCTORS, *Applied Physics Letters* **1**, 7 (1962), <https://doi.org/10.1063/1.1777362>.
- [43] A. M. Clogston, Upper Limit for the Critical Field in Hard Superconductors, *Phys. Rev. Lett.* **9**, 266 (1962).
- [44] Y. Matsuda and H. Shimahara, Fulde-Ferrell-Larkin-Ovchinnikov State in Heavy Fermion Superconductors, *Journal of the Physical Society of Japan* **76**, 051005 (2007), <https://doi.org/10.1143/JPSJ.76.051005>.
- [45] A. Ramires and M. Sigrist, Identifying detrimental effects for multiorbital superconductivity: Application to Sr₂RuO₄, *Phys. Rev. B* **94**, 104501 (2016).
- [46] A. Ramires, D. F. Agterberg, and M. Sigrist, Tailoring T_c by symmetry principles: The concept of superconducting fitness, *Phys. Rev. B* **98**, 024501 (2018).
- [47] G. Sarma, On the influence of a uniform exchange field acting on the spins of the conduction electrons in a superconductor,

- Journal of Physics and Chemistry of Solids **24**, 1029 (1963).
- [48] K. Maki and T. Tsuneto, Pauli Paramagnetism and Superconducting State, Progress of Theoretical Physics **31**, 945 (1964), <https://academic.oup.com/ptp/article-pdf/31/6/945/5271369/31-6-945.pdf>
- [49] F. S. Bergeret, A. F. Volkov, and K. B. Efetov, Long-Range Proximity Effects in Superconductor-Ferromagnet Structures, Phys. Rev. Lett. **86**, 4096 (2001).
- [50] Y. Noda, K. Ohno, and S. Nakamura, Momentum-dependent band spin splitting in semiconducting MnO₂: a density functional calculation, Phys. Chem. Chem. Phys. **18**, 13294 (2016).
- [51] T. Okugawa, K. Ohno, Y. Noda, and S. Nakamura, Weakly spin-dependent band structures of antiferromagnetic perovskite LaMO₃ (M = Cr, Mn, Fe), Journal of Physics: Condensed Matter **30**, 075502 (2018).
- [52] L. Šmejkal, R. González-Hernández, T. Jungwirth, and J. Sinova, Crystal time-reversal symmetry breaking and spontaneous Hall effect in collinear antiferromagnets, Science Advances **6**, eaaz8809 (2020), <https://www.science.org/doi/pdf/10.1126/sciadv.aaz8809>.
- [53] M. Naka, S. Hayami, H. Kusunose, Y. Yanagi, Y. Motome, and H. Seo, Spin current generation in organic antiferromagnets, Nature Communications **10**, 4305 (2019).
- [54] K.-H. Ahn, A. Hariki, K.-W. Lee, and J. Kuneš, Antiferromagnetism in RuO₂ as *d*-wave Pomeranchuk instability, Phys. Rev. B **99**, 184432 (2019).
- [55] S. Hayami, Y. Yanagi, and H. Kusunose, Momentum-Dependent Spin Splitting by Collinear Antiferromagnetic Ordering, Journal of the Physical Society of Japan **88**, 123702 (2019), <https://doi.org/10.7566/JPSJ.88.123702>.
- [56] S. Hayami, Y. Yanagi, M. Naka, H. Seo, Y. Motome, and H. Kusunose, Multipole Description of Emergent Spin-Orbit Interaction in Organic Antiferromagnet κ -(BEDT-TTF)₂Cu[N(CN)₂]Cl, JPS Conf. Proc. **30**, 011149 (2020), <https://journals.jps.jp/doi/pdf/10.7566/JSPSC.30.011149>.
- [57] S. Hayami, Y. Yanagi, and H. Kusunose, Bottom-up design of spin-split and reshaped electronic band structures in antiferromagnets without spin-orbit coupling: Procedure on the basis of augmented multipoles, Phys. Rev. B **102**, 144441 (2020).
- [58] L.-D. Yuan, Z. Wang, J.-W. Luo, E. I. Rashba, and A. Zunger, Giant momentum-dependent spin splitting in centrosymmetric low-*Z* antiferromagnets, Phys. Rev. B **102**, 014422 (2020).
- [59] M. Naka, Y. Motome, and H. Seo, Perovskite as a spin current generator, Phys. Rev. B **103**, 125114 (2021).
- [60] L.-D. Yuan, Z. Wang, J.-W. Luo, and A. Zunger, Prediction of low-*Z* collinear and noncollinear antiferromagnetic compounds having momentum-dependent spin splitting even without spin-orbit coupling, Phys. Rev. Mater. **5**, 014409 (2021).
- [61] L.-D. Yuan, Z. Wang, J.-W. Luo, and A. Zunger, Strong influence of nonmagnetic ligands on the momentum-dependent spin splitting in antiferromagnets, Phys. Rev. B **103**, 224410 (2021).
- [62] R. González-Hernández, L. Šmejkal, K. Výborný, Y. Yahagi, J. Sinova, T. c. v. Jungwirth, and J. Železný, Efficient Electrical Spin Splitter Based on Nonrelativistic Collinear Antiferromagnetism, Phys. Rev. Lett. **126**, 127701 (2021).
- [63] L. Šmejkal, A. B. Hellenes, R. González-Hernández, J. Sinova, and T. Jungwirth, Giant and Tunneling Magnetoresistance in Unconventional Collinear Antiferromagnets with Nonrelativistic Spin-Momentum Coupling, Phys. Rev. X **12**, 011028 (2022).
- [64] I. I. Mazin, K. Koepernik, M. D. Johannes, R. González-Hernández, and L. Šmejkal, Prediction of unconventional magnetism in doped FeSb₂, Proceedings of the National Academy of Sciences **118**, e2108924118 (2021).
- [65] L. Šmejkal, J. Sinova, and T. Jungwirth, Beyond Conventional Ferromagnetism and Antiferromagnetism: A Phase with Nonrelativistic Spin and Crystal Rotation Symmetry, Phys. Rev. X **12**, 031042 (2022).
- [66] L. Šmejkal, J. Sinova, and T. Jungwirth, Emerging Research Landscape of Altermagnetism, Phys. Rev. X **12**, 040501 (2022).
- [67] S.-W. Cheong and F.-T. Huang, Altermagnetism classification, npj Quantum Materials **10**, 38 (2025).
- [68] Z. Guo, X. Wang, W. Wang, G. Zhang, X. Zhou, and Z. Cheng, Spin-Polarized Antiferromagnets for Spintronics, Advanced Materials, 2505779 (2025).
- [69] M. Hu, X. Cheng, Z. Huang, and J. Liu, Catalog of *C*-Paired Spin-Momentum Locking in Antiferromagnetic Systems, Phys. Rev. X **15**, 021083 (2025).
- [70] L. P. Gor'kov and E. I. Rashba, Superconducting 2D System with Lifted Spin Degeneracy: Mixed Singlet-Triplet State, Phys. Rev. Lett. **87**, 037004 (2001).
- [71] P. A. Frigeri, D. F. Agterberg, A. Koga, and M. Sigrist, Superconductivity without Inversion Symmetry: MnSi versus CePt₃Si, Phys. Rev. Lett. **92**, 097001 (2004).
- [72] P. A. Frigeri, D. F. Agterberg, and M. Sigrist, Spin susceptibility in superconductors without inversion symmetry, New Journal of Physics **6**, 115 (2004).
- [73] The odd-order terms would play an important role in discussing other exotic phenomena, such as the superconducting diode effect [6–8]. The effects of these terms will be discussed elsewhere.
- [74] D. Chakraborty and A. M. Black-Schaffer, Interplay of finite-energy and finite-momentum superconducting pairing, Phys. Rev. B **106**, 024511 (2022).
- [75] A. A. Abrikosov, L. P. Gor'kov, and I. E. Dzyaloshinski, *Methods of Quantum Field Theory in Statistical Physics* (Dover Publications, New York, 1975).
- [76] M. Tinkham, *Introduction to Superconductivity* (McGraw-Hill, New York, 1996).
- [77] H. Burkhardt and D. Rainer, Fulde-Ferrell-Larkin-Ovchinnikov state in layered superconductors, Annalen der Physik **506**, 181 (1994).
- [78] H. Shimahara, Fulde-Ferrell state in quasi-two-dimensional superconductors, Phys. Rev. B **50**, 12760 (1994).
- [79] H. Shimahara, Fulde-Ferrell-Larkin-Ovchinnikov State in a Quasi-Two-Dimensional Organic Superconductor, Journal of the Physical Society of Japan **66**, 541 (1997), <https://doi.org/10.1143/JPSJ.66.541>.
- [80] T. Yokoyama, S. Onari, and Y. Tanaka, Theory of Fulde-Ferrell-Larkin-Ovchinnikov State of Superconductors with and without Inversion Symmetry: Hubbard Model Approach, Journal of the Physical Society of Japan **77**, 064711 (2008), <https://doi.org/10.1143/JPSJ.77.064711>.
- [81] H. Shimahara, S. Matsuo, and K. Nagai, Nonuniform superconductivity due to the orbital magnetic ef-

- fect in a d-wave superconductor in a magnetic field, Phys. Rev. B **53**, 12284 (1996).
- [82] J. M. Luttinger and W. Kohn, Motion of Electrons and Holes in Perturbed Periodic Fields, Phys. Rev. **97**, 869 (1955).
- [83] M. Sigrist and K. Ueda, Phenomenological theory of unconventional superconductivity, Rev. Mod. Phys. **63**, 239 (1991).
- [84] D. F. Agterberg, P. M. R. Brydon, and C. Timm, Bogoliubov Fermi Surfaces in Superconductors with Broken Time-Reversal Symmetry, Phys. Rev. Lett. **118**, 127001 (2017).
- [85] P. M. R. Brydon, D. F. Agterberg, H. Menke, and C. Timm, Bogoliubov Fermi surfaces: General theory, magnetic order, and topology, Phys. Rev. B **98**, 224509 (2018).
- [86] B. Roy, S. A. A. Ghorashi, M. S. Foster, and A. H. Nevidomskyy, Topological superconductivity of spin-3/2 carriers in a three-dimensional doped Luttinger semimetal, Phys. Rev. B **99**, 054505 (2019).
- [87] D. Kim, S. Kobayashi, and Y. Asano, Quasiparticle on Bogoliubov Fermi Surface and Odd-Frequency Cooper Pair, Journal of the Physical Society of Japan **90**, 104708 (2021).
- [88] P. Dutta, F. Parhizgar, and A. M. Black-Schaffer, Superconductivity in spin-3/2 systems: Symmetry classification, odd-frequency pairs, and Bogoliubov Fermi surfaces, Phys. Rev. Res. **3**, 033255 (2021).
- [89] J. Nagamatsu, N. Nakagawa, T. Muranaka, Y. Zenitani, and J. Akimitsu, Nature (London) **410**, 63 (2001).
- [90] H. J. Choi, D. Roundy, H. Sun, M. L. Cohen, and S. G. Louie, Nature (London) **418**, 758 (2002).
- [91] Y. Kamihara, T. Watanabe, M. Hirano, and H. Hosono, J. Am. Chem. Soc. **130**, 3296 (2008).
- [92] K. Kuroki, S. Onari, R. Arita, H. Usui, Y. Tanaka, H. Kontani, and H. Aoki, Unconventional Pairing Originating from the Disconnected Fermi Surfaces of Superconducting $\text{LaFeAsO}_{1-x}\text{F}_x$, Phys. Rev. Lett. **101**, 087004 (2008).
- [93] A. Sasaki, S. Ikegaya, T. Habe, A. A. Golubov, and Y. Asano, Josephson effect in two-band superconductors, Phys. Rev. B **101**, 184501 (2020).
- [94] L. Fu and E. Berg, Odd-Parity Topological Superconductors: Theory and Application to $\text{Cu}_x\text{Bi}_2\text{Se}_3$, Phys. Rev. Lett. **105**, 097001 (2010).
- [95] K. Matano, M. Kriener, K. Segawa, Y. Ando, and G.-q. Zheng, Spin-rotation symmetry breaking in the superconducting state of $\text{Cu}_x\text{Bi}_2\text{Se}_3$, Nat. Phys. **12**, 852 (2016).
- [96] S. Nakosai, Y. Tanaka, and N. Nagaosa, Topological Superconductivity in Bilayer Rashba System, Phys. Rev. Lett. **108**, 147003 (2012).
- [97] T. Sato and Y. Asano, Superconductivity in Cu-doped Bi_2Se_3 with potential disorder, Phys. Rev. B **102**, 024516 (2020).
- [98] T. Mizushima, S. Tamura, K. Yada, and Y. Tanaka, Odd-frequency pairs and anomalous proximity effect in nematic and chiral states of superconducting topological insulators, Phys. Rev. B **107**, 064504 (2023).
- [99] Y. Saito, Y. Nakamura, M. S. Bahramy, Y. Kohama, J. Ye, Y. Kasahara, Y. Nakagawa, M. Onga, M. Tokunaga, T. Nojima, *et al.*, Superconductivity protected by spin-valley locking in ion-gated MoS_2 , Nature Physics **12**, 144 (2016).
- [100] X. Xi, Z. Wang, W. Zhao, J.-H. Park, K. T. Law, H. Berger, L. Forró, J. Shan, and K. F. Mak, Ising pairing in superconducting NbSe_2 atomic layers, Nature Physics **12**, 139 (2016).
- [101] S. C. De la Barrera, M. R. Sinko, D. P. Gopalan, N. Sivadas, K. L. Seyler, K. Watanabe, T. Taniguchi, A. W. Tsen, X. Xu, D. Xiao, *et al.*, Tuning Ising superconductivity with layer and spin-orbit coupling in two-dimensional transition-metal dichalcogenides, Nature communications **9**, 1427 (2018).
- [102] D. C. Cavanagh, D. F. Agterberg, and P. M. R. Brydon, Pair breaking in superconductors with strong spin-orbit coupling, Phys. Rev. B **107**, L060504 (2023).
- [103] It is not possible to carry out the integration over momenta analytically in Eq. (A19) in many cases. In such cases, Q in Eq. (68) can be replaced by $Q^{\mathcal{F}}$, which corresponds to the contribution of the anomalous Green's function to the superfluid density.
- [104] Of course, this argument is not valid when the electron correlations in the normal state are very strong [77]. However, the relation is expected to hold in most weak-coupling SCs.
- [105] E. Taylor, A. Griffin, N. Fukushima, and Y. Ohashi, Pairing fluctuations and the superfluid density through the BCS-BEC crossover, Phys. Rev. A **74**, 063626 (2006).
- [106] R. Peierls, Zur Theorie des Diamagnetismus von Leitungselektronen., Z. Physik **80**, 763 (1933).
- [107] J. M. Luttinger, The Effect of a Magnetic Field on Electrons in a Periodic Potential, Phys. Rev. **84**, 814 (1951).
- [108] D. J. Scalapino, S. R. White, and S. C. Zhang, Superfluid density and the Drude weight of the Hubbard model, Phys. Rev. Lett. **68**, 2830 (1992).
- [109] D. J. Scalapino, S. R. White, and S. Zhang, Insulator, metal, or superconductor: The criteria, Phys. Rev. B **47**, 7995 (1993).
- [110] T. Kostyrko, R. Micnas, and K. A. Chao, Gauge-invariant theory of the Meissner effect in the lattice model of a superconductor with local pairing, Phys. Rev. B **49**, 6158 (1994).